




PAPER

[View Article Online](#)
[View Journal](#) | [View Issue](#)Cite this: *Dalton Trans.*, 2025, **54**, 2301

Donor-free 9-aluminafluorenes: molecular structures and reactivity†

Paula L. Lückert, Jannik Gilmer, Alexander Virovets,  Hans-Wolfram Lerner  and Matthias Wagner *

Aluminum-doped polycyclic aromatic hydrocarbons (PAHs) are underexplored despite the broad applications of boron-containing PAHs in areas such as catalysis and optoelectronics. We disclose the donor-free, sterically unprotected 9-methyl-9-aluminafluorene (Me-AlFlu; **2**), synthesized by heating a 9,9-dimethyl-9-stannafluorene and AlMe₃ in hexanes. The compound is a dimer, (**2**)₂, with *trans*-positioned AlMe substituents in the solid state. In solution, (**2**)₂ shows a dynamic *cis/trans*-interconversion rather than a monomer-dimer equilibrium (Tol-*d*₈, RT). Lewis bases L cleave (**2**)₂ into monomeric adducts **2**·L (L = OEt₂, thf, pyridine). Lewis acidic AlBr₃ transforms (**2**)₂ into a 2,2'-(Br₂Al)₂-1,1'-biphenyl (**3**), crystallographically characterized as dimeric (**3**)₂. (**3**)₂ is a synthetic equivalent for the elusive free Br-AlFlu: Treatment with donor molecules furnishes Br-AlFlu·L adducts (L = OEt₂, pyridine); the three-coordinate, monomeric aluminafluorene Mes*–AlFlu was prepared from (**3**)₂, Mes*Li, and a 2,2'-dilithio-1,1'-biphenyl in quantitative yield (Mes* = 2,4,6-(*t*Bu)₃C₆H₂).

Received 11th November 2024,
Accepted 29th November 2024

DOI: 10.1039/d4dt03148b

rsc.li/dalton

Introduction

Doping organic π -electron systems with other p-block elements is an effective strategy to impart new chemical and physical properties to these species.¹ Specifically, the combination of a polycyclic aromatic hydrocarbon (PAH) such as fluorene with boron as a dopant to generate 9-borafluorenes (BFlus) can have a particularly pronounced effect,^{2,3} as a conjugation barrier (*i.e.*, the CH₂ fragment in the carbonaceous species) is removed and a vacant B(p_z) orbital is introduced instead, which can now: (i) mediate electron delocalization and bring about novel optoelectronic properties,⁴ (ii) facilitate reduction,^{5,6} and (iii) act as a Lewis acid to promote bond-activation reactions⁷ or the expansion of the five-membered central borole ring.⁸

Compared to the extensive research on BFlus, their heavier homologues, the 9-aluminafluorenes (AlFlus),^{9,10} are far less well explored. This is unfortunate, because AlFlus are expected to exhibit a lower degree of aryl-heteroatom double-bond character than BFlus,¹¹ leading to a greater propensity to form structurally intriguing aggregates through Al $\cdots\pi$ (Ar) complexes

or Al–C–Al' two-electron–three-center (2e3c) bonds. Relative to open-chain arylaluminum compounds, AlFlus should possess a structurally enforced enhanced Lewis acidity due to their small endohedral C–Al–C angle. This angle (108° in a regular five-membered ring) deviates more from the ideal 120° angle of three-coordinate AlR₃ species than from the corresponding angles of perfectly tetrahedral (109.5°) adducts. By the same token, the behavior of Al-based Lewis acids is more diverse than that of their B-based counterparts, as Al sites, unlike B centers, can readily accommodate coordination numbers larger than four.

In 1962, Eisch *et al.* reported the formation of Ph-AlFlu through the metalative cyclization of *o*-biphenyl(diphenyl) aluminum at 200 °C. Their claim was mainly based on the analysis of hydrolysis and iodinolysis products.^{12,13} The topic lay dormant until 2015, when Chujo and Tanaka used salt-metalathesis protocols to synthesize AlFlus carrying Al-bonded phenyl rings with one or two chelating (dimethylamino)methyl substituents at their *ortho* positions (Fig. 1). Their research focused on the emission properties of the obtained four- and five-coordinate AlFlus.^{14,15} More recently, Braunschweig *et al.* disclosed the synthesis of various aluminafluorenes R-AlFlu [R = 1,2,4-(*t*Bu)₃C₅H₂ (92%; Fig. 1), Ph₂(*t*Bu)Si (44%), 2-C₄H₃S (79%), *t*Bu (23%; Fig. 1), Br (53%)]. The compounds were again prepared from 2,2'-dilithio-1,1'-biphenyl by salt-metalathesis reactions and isolated and structurally characterized as their ether adducts – with the exception of the η^5 -cyclopentadienide derivative, which is monomeric in the solid state, and the *t*Bu derivative, which crystallizes as a dimer.¹⁶

Institut für Anorganische und Analytische Chemie, Goethe-Universität Frankfurt,
Max-von-Laue-Straße 7, D-60438 Frankfurt, Main, Germany.

E-mail: matthias.wagner@chemie.uni-frankfurt.de

†Electronic supplementary information (ESI) available: Synthetic procedures, NMR spectra, X-ray crystallographic data and computational details. CCDC 2394332–2394341. For ESI and crystallographic data in CIF or other electronic format see DOI: <https://doi.org/10.1039/d4dt03148b>

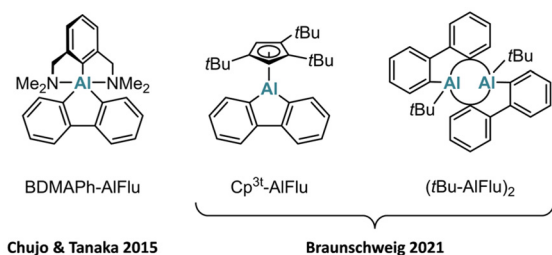


Fig. 1 Known mono- and dimeric 9-aluminafluorenes featuring 2,6-bis[(dimethylamino)methyl]phenyl (BDMAPh), 1,2,4-(*t*Bu)₃C₅H₂ (Cp^{3t}), and *tert*-butyl (*t*Bu) substituents.

One aim of our study outlined herein was to develop straightforward, high-yield synthesis protocols for base-free R-AlFlus featuring (i) the small substituent R = Me to minimize steric shielding of the Al center, and (ii) the reactive substituent R = Br for late-stage derivatization. Particular emphasis was placed on the molecular structure of Me-AlFlu in non-donor solvents and in the solid state, as well as on the synthesis of the first base-free, three-coordinate, monomeric aluminafluorene, Mes^{*}-AlFlu (Mes^{*} = 2,4,6-(*t*Bu)₃C₆H₂). All our AlFlus were equipped with *t*Bu groups in their 2,7-positions to enhance solubility in non-polar solvents and to facilitate NMR-spectroscopic analysis.

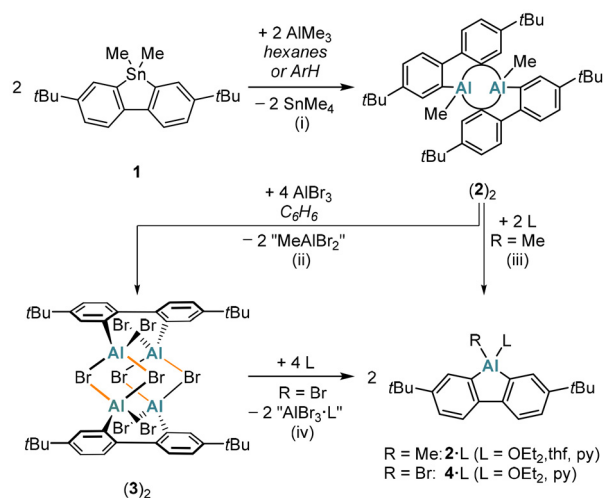
Results and discussion

Syntheses

The base-free Me-AlFlu (**2**) was synthesized by heating the 9,9-dimethyl-9-stannafluorene **1** with 1 equiv. of AlMe₃¹⁷ in either hexanes or C₆H₆/toluene (Scheme 1). The only by-product formed is the volatile and relatively inert SnMe₄.^{18,19} An advantage of using hexanes as the solvent is that the dimer (**2**)₂ precipitates in pure form already upon cooling the reaction mixture to room temperature (yield: 74%); when C₆H₆/toluene is employed, the yield of (**2**)₂ is higher (91%), but some further workup is required. In the presence of the donor molecules Et₂O, THF, or pyridine, (**2**)₂ is cleanly split into its constituting monomers to furnish the monoadducts 2-OEt₂, 2-thf, or 2-py (Scheme 1).

Treatment of (**2**)₂ with 4 equiv. of AlBr₃¹⁷ in C₆H₆ results not only in quantitative AlMe/AlBr exchange but also in the incorporation of two AlBr₃ molecules to afford dimeric 2,2'-(Br₂Al)₂-1,1'-biphenyl [(**3**)₂, 95%; Scheme 1]. Upon addition of Et₂O to (**3**)₂ in C₆H₆, the donor adduct of Br-AlFlu, 4-OEt₂, precipitates quantitatively as a colorless solid. In terms of yield, our overall synthesis cascade to 4-OEt₂ improves upon the published protocol¹⁶ by about 40 percentage points. Although pyridine can also reconstitute the AlFlu scaffold from (**3**)₂, it proved challenging to separate the target product 4-py from by-products such as [AlBr₂(py)₄][X] ([**5**][X]; X = Br[−], AlBr₄[−]; Fig. S44 and S45†).

A particularly notable application of (**3**)₂ as a synthetic equivalent of donor-free Br-AlFlu is the preparation of Mes^{*}-AlFlu

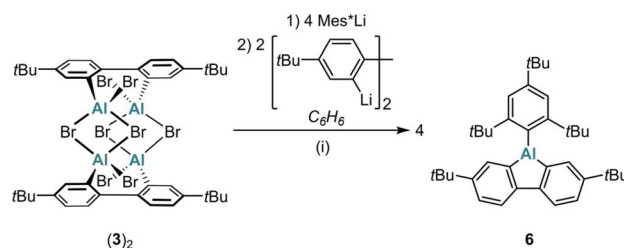


Scheme 1 Synthesis of donor-free (**2**)₂ through Sn/Al exchange between the 9-stannafluorene **1** and AlMe₃ (ArH: C₆H₆/toluene). The addition of AlBr₃ to (**2**)₂ furnishes (**3**)₂. Lewis bases (L: Et₂O, THF, or pyridine), cleave (**2**)₂ or (**3**)₂ into the monomeric adducts 2-L or 4-L. (i) Hexanes, 140 °C, 3 d (74% yield) or C₆H₆/toluene, 120 °C, 3 d (91% yield); sealed glass ampoule. (ii) C₆H₆, room temperature, 1 d (95% yield). (iii) 2-OEt₂: in Et₂O, room temperature; 2-thf: C₆D₆, room temperature; 2-py: C₆H₆, room temperature (quantitative conversions). (iv) 4-OEt₂: C₆H₆, room temperature (quantitative conversion); 4-py: C₆D₆, room temperature (not isolated). Note: in (**3**)₂, four bonds were arbitrarily chosen as formally intermolecular (highlighted in orange) to facilitate the distinction between the monomers M and M'.

(**6**): sequential addition of Mes^{*}Li (4 equiv.) and 2,2'-dilithio-4,4'-di-*tert*-butyl-1,1'-biphenyl (2 equiv.) to (**3**)₂ in C₆H₆ gave **6** in 97% yield (Scheme 2).

Solid-state structures

In the solid state, Me-AlFlu forms centrosymmetric dimers, with the Al-bonded Me substituents adopting a *trans*-configuration (*trans*-(**2**)₂; Fig. 2).²⁰ The individual monomers, M and M', are linked by two Al...C interactions, resulting in two Al(1) ...Al(1') bridging aryl rings (Ar_b) and two terminal rings (Ar_t), with bridging [C(11)] and terminal [C(21)] *ipso*-C atoms. The position of Ar_b is asymmetric between Al(1) and Al(1'), as indicated by the differing angles Al(1)–C(11) ... C(14) = 153.13(17)° and Al(1')–C(11) ... C(14) = 128.38(16)°. The fact that the



Scheme 2 Synthesis of Mes^{*}-AlFlu (**6**) using (**3**)₂ as a synthetic equivalent of the elusive Br-AlFlu. (i) C₆H₆, room temperature, 1 d (97% yield).



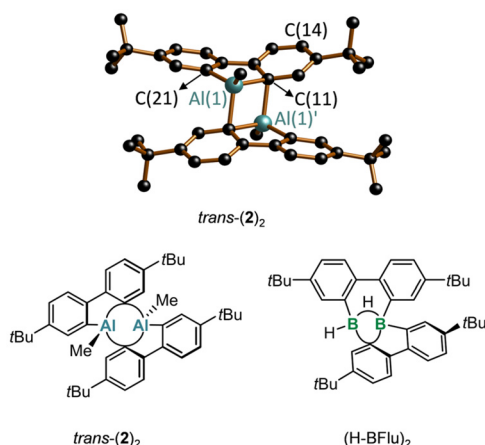


Fig. 2 Top: molecular structure of *trans*-(**2**)₂ in the solid state; H atoms omitted for clarity (C: black, Al: turquoise). Bottom: structural formulae of *trans*-(**2**)₂ and of the comparable 9-borafluorene dimer (H-BFlu)₂.

Al(1)′–C(11)–C(14) angle is significantly closer to 90° than the Al(1)–C(11)–C(14) angle can still be viewed as a remnant of the initial intermolecular Al⋯π(Ar) complex when the two heterofluorene units first encountered each other. Correspondingly, the ‘intermonomer’ Al(1)′–C(11) bond (2.148(3) Å) is longer by 0.055 Å than the ‘intramonomer’ Al(1)–C(11) bond (2.093(3) Å; *cf.* Al(1)–C(21) = 1.971(3) Å). The range of C–C bond lengths in Ar_b (1.382(5)–1.427(5) Å) is close to that in Ar_t (1.389(5)–1.409(5) Å), indicating that the bridging mode does not lead to a systematic bond-length alternation. However, the two C–C bonds involving the bridging C(11) atom are slightly longer than the other four (1.409(4) and 1.427(5) Å *vs.* 1.382(5)–1.401(5) Å). Finally, we note that *trans*-(**2**)₂ has very similar structural parameters to Braunschweig’s (tBu-AlFlu)₂,¹⁶ while the comparable 9-borafluorene dimer (H-BFlu)₂ shows one B–(μ-H)–B two-electron–three-center bond and one B⋯B′-bridging aryl ring (the three other rings remain terminally bonded).²¹

X-ray crystallography reveals that the compound (**3**)₂ no longer contains the 9-aluminafluorene motif but instead forms a centrosymmetric 2,2′-(Br₂Al)₂-1,1′-biphenyl dimer (Fig. 3).

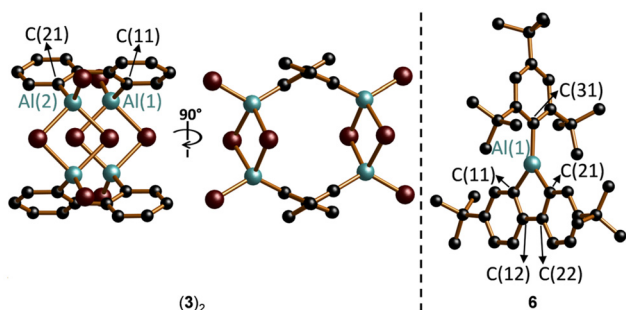


Fig. 3 Left: molecular structure of (**3**)₂ in the solid state, viewed from two different perspectives; tBu-groups in the 2,7-positions of the biphenyl backbones and H atoms omitted for clarity. Right: molecular structure of **6** in the solid state; H atoms omitted for clarity (C: black, Al: turquoise, Br: brown).

The two Br₂Al substituents in each monomer adopt an approximate *s-trans* configuration with a torsion angle Al(1)–C(11)–C(21)–Al(2) of 129.55(19)° [Al(1)–C(11) = 1.945(5) Å, Al(2)–C(21) = 1.956(4) Å]. Four Br atoms occupy bridging positions between Al centers of different monomers, assembling the cage-like structure of (**3**)₂. The underlying structural feature, a four-membered R(Br)Al–(μ-Br)₂–Al(Br)R ring, is common not only for aluminum tribromide (R = Br) but also for numerous dibromo(organo)alanes.²²

The 2,4,6-(tBu)₃C₆H₂-substituted Mes*–AlFlu (**6**) exists as a monomeric species with a three-coordinate Al center in the crystal lattice (Fig. 3). The sum of C–Al–C angles is 360°, confirming a trigonal-planar ligand environment, although the endocyclic C(11)–Al(1)–C(21) bond angle is nearly rectangular (91.79(6)°). All three Al–C bonds are of equal length, regardless of whether they are endo- or exocyclic, or whether the respective *ipso*-C(*p_z*) orbital is positioned parallel or orthogonal to the vacant Al(*p_z*) orbital [Al(1)–C(11)/C(21)/C(31) = 1.9611(14)/1.9516(14)/1.9606(13) Å]. Within the five-membered AlC₄ core, the length of the central C(12)–C(22) bond (1.5024(19) Å) approaches that of a typical C–C single bond (1.54 Å),²³ while the benzannulated bonds are significantly shorter [C(11)–C(12)/C(21)–C(22) = 1.4208(18)/1.4134(18) Å]. The other ten C–C bonds within the biphenyl fragment fall within a narrow range of 1.389(2)–1.4041(19) Å, closely matching the corresponding bonds in C₆H₆ (1.39 Å).²⁴ Taken together, this analysis of bond lengths suggests that the AlFlu moiety of **6** preserves two largely unperturbed Clar sextets within its two C₆H₃ fragments, with no indication of a delocalized (antiaromatic) π-system, nor any significant Al(1)=C(11)/C(21) double-bond character in the AlC₄ heterocycle.

The donor adducts 2-OEt₂, 2-py, and 4-py were subjected to X-ray analysis to confirm that (**2**)₂ and (**3**)₂ can indeed serve as precursors of Me-AlFlu and Br-AlFlu, respectively (Fig. S40, S41, S43†). Furthermore, compared to donor-free **6**, the C–C bond lengths within the C₆H₃–C₆H₃ units of 2-py and 4-py were found to differ by no more than 3σ (and much less for most bonds).²⁵ This observation again suggests that the vacant Al(*p_z*) orbital exerts no significant electron-withdrawing mesomeric effect on the π-electron system.

NMR analysis

At room temperature, **2** gives severely broadened ¹H NMR signals, providing limited diagnostic value (Tol-*d*₈; Fig. 4 and S7†). At 70 °C, two sharp resonances are detectable in the aliphatic region of the spectrum (integral ratio 3H : 18H); the aromatic region contains one broad feature and two doublets with coupling constants of about 8.2 Hz (Fig. 4 and S6†). At –30 °C, the ¹H NMR spectrum of **2** is characterized by two well-resolved sets of signals attributable to two different but closely similar components (Fig. 4 and S8†); the same is true for the ¹³C{¹H} NMR spectrum (Fig. S9†). The proton-integral values of the two sets indicate a minor-to-major component ratio of approximately 0.12 : 1 (Fig. S8†). Focusing on the major component, the ¹H NMR spectrum reveals one singlet at –0.67 ppm (6H), and two additional singlets at 1.47 and



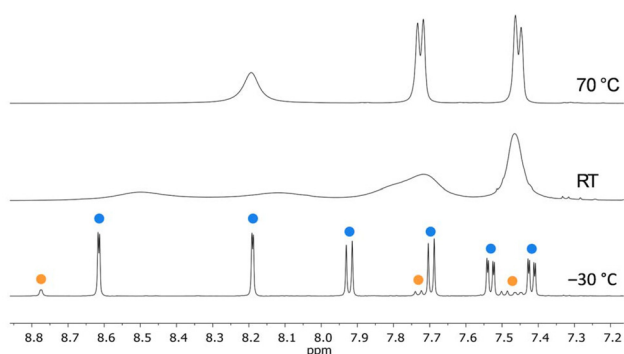


Fig. 4 Aromatic regions of ^1H NMR spectra of $(2)_2$ in Tol- d_8 (500.2 MHz). Top: 70 °C. Middle: room temperature. Bottom: –30 °C. ●: *trans*-(2) $_2$. ●: *cis*-(2) $_2$.

1.28 ppm ($2 \times 18\text{H}$), assignable to two equivalent AlMe substituents and two pairs of non-equivalent *t*Bu groups, respectively. In the aromatic region, four doublets ($4 \times 2\text{H}$; $2 \times {}^3J_{\text{H,H}} = 8.2\text{ Hz}$, $2 \times {}^4J_{\text{H,H}} = 2.2\text{ Hz}$) and two doublets of doublets ($2 \times 2\text{H}$) are observed, indicative of two pairs of non-equivalent C_6H_3 fragments. In principle, these NMR features would align with both the molecular structure of the *cis*- and *trans*-(2) $_2$ dimer (as observed in the solid state). *Vice versa*, the minor signal set likely arises from *trans*- or *cis*-(2) $_2$. At low temperatures, both isomers are present in an (essentially) static mixture, while some dynamic rearrangement equilibrium is established at higher temperatures. This preliminary conclusion raises two questions: (i) Does *cis*- or *trans*-(2) $_2$ dominate at low temperatures? (ii) Is the dynamic equilibrium at high temperatures due to monomer/dimer association/dissociation, or is it the result of a rapidly interconverting *cis/trans* dimeric form of $(2)_2$?

To address question (i), quantum-chemical calculations predict that the crystallographically characterized *trans*-(2) $_2$ is 1.6 kcal mol $^{-1}$ more favorable in energy than *cis*-(2) $_2$ (Scheme S1†; experimental value, determined at –30 °C from the proton-integral values of the minor/major component: $\Delta G^\circ = 0.7\text{ kcal mol}^{-1}$). Furthermore, the relative proportion of the minor component increases with solvent polarity, consistent with the existing dipole moment of *cis*-(2) $_2$ (^1H NMR spectroscopic control; Table S1 and Fig. S1, S2†). Finally, the computed ^{13}C chemical shift values for *cis/trans*-(2) $_2$ align more closely with the assumption that the major component is *trans*-(2) $_2$ rather than *vice versa* (Tables S9–S11†). It is therefore safe to assume that the major component in an equilibrating *cis/trans*-(2) $_2$ mixture is the *trans* isomer.

Regarding question (ii), we note that the computed energy required for cleaving *trans*-(2) $_2$ into its constituting monomers is 19.4 kcal mol $^{-1}$ (in CH_2Cl_2). In contrast, the computed energy barrier of the *cis/trans* interconversion of $(2)_2$ is only $\Delta G^\ddagger = 14.8\text{ kcal mol}^{-1}$, which agrees well with the value of $\approx 14.5\text{ kcal mol}^{-1}$ experimentally determined from the coalescence temperature (T_c) in conjunction with the maximum peak separation ($\Delta\nu$) in the slow-exchange limit (CD_2Cl_2 ; see the

ESI† for full details). The observed NMR features are therefore more convincingly attributed to a dynamic *cis/trans* equilibrium rather than to a monomer/dimer association/dissociation equilibrium.

In the temperature range of –30 to 70 °C, $(3)_2$ exhibited only extremely broadened signals in the ^1H and $^{13}\text{C}\{^1\text{H}\}$ NMR spectra, providing no structural information.

The ^1H and $^{13}\text{C}\{^1\text{H}\}$ NMR spectra of all adducts formed between our R-AlFlu and Lewis bases are in accord with the proposed molecular structures, as is the case for ligand-free **6** (see the ESI† for the fully assigned spectra). In addition to aiding in structure elucidation, $^{13}\text{C}\{^1\text{H}\}$ NMR spectroscopy is also a valuable tool for mapping the π -charge density distribution in conjugated systems, as the shielding of a specific $\text{C}(\text{sp}^2)$ atom depends linearly on the corresponding π -electron density at that position.²⁶ Given this background, we compared the ^{13}C chemical shift values of the C atoms constituting the C_6H_3 – C_6H_3 fragment of **6** with those of the equivalent atoms in the corresponding fragments of the adducts 2-OEt $_2$, 2-thf, 2-py, 4-OEt $_2$, and 4-py. Except for the Al-bonded *ipso*-C atoms, whose shift differences varied from $\delta(\text{6}) - \delta(\text{adduct}) = 3.3$ to –4.7 ppm without a systematic trend, the $\Delta\delta(^{13}\text{C})$ values for all other structurally analogous C atoms were less than $\pm 1.8\text{ ppm}$. In other words, we found no evidence of an overall ^{13}C -deshielding effect or π -electron depletion in **6** that could be attributed to a mesomerically electron-withdrawing $\text{Al}(\text{sp}^2)$ center.

$^{13}\text{C}\{^1\text{H}\}$ NMR spectroscopy on 2-py and 4-py provides a method to evaluate the relative Lewis acidities of free, monomeric Me-AlFlu and Br-AlFlu: in pyridine complexes of main-group elements, stronger acids induce increased shielding of the C-2,6 and deshielding of the C-3,4,5 nuclei of the ligand.²⁷ For 2-py/4-py, our observations consistently indicate that Me-AlFlu is the stronger acid, comparable in this respect to BPh_3 .²⁸ X-ray crystallography, however, offers a contrasting view: 4-py exhibits a shorter Al–N bond and a more pyramidalized Al center, implying higher Lewis acidity for Br-AlFlu.²⁸ Given the small differences in the key NMR and structural parameters between 2-py and 4-py, these conflicting observations highlight the limitation of relying on a single method to determine Lewis acidity, emphasizing the need for complementary approaches.

Conclusions

We synthesized the donor-free 9-aluminafluorene Me-AlFlu (**2**), which was characterized as its dimer $(2)_2$ through X-ray crystallography and VT NMR spectroscopy (Tol- d_8). The key to this success was the highly selective reaction between the 9,9-dimethyl-9-stannafluorene **1** and AlMe_3 ,^{17,18} which proceeds in non-donor solvents and releases volatile SnMe_4 as the sole by-product. Unlike the bulky *tert*-butyl group in *t*Bu-AlFlu,¹⁶ the sterically less demanding methyl substituent in Me-AlFlu allows relatively unhindered access to the electrophilic Al center, as demonstrated by the straightforward formation of



Dalton Trans., 2025, 54, 2301-2307 | 2305

- 9H-9-Borafluorene, *Organometallics*, 2013, **32**, 6827–6833; (c) J. Gilmer, T. Trageser, L. Čaić, A. Virovets, M. Bolte, H.-W. Lerner, F. Fantuzzi and M. Wagner, Catalyst-free diboration and silaboration of alkenes and alkynes using bis(9-heterofluorenyl)s, *Chem. Sci.*, 2023, **14**, 4589–4596; (d) J. Gilmer, M. Bolte, A. Virovets, H.-W. Lerner, F. Fantuzzi and M. Wagner, A Hydride-Substituted Homoleptic Silylborate: How Similar is it to its Diborane(6)-Dianion Isostere?, *Chem. – Eur. J.*, 2023, **29**, e202203119.
- 8 (a) A. Hübner, Z.-W. Qu, U. Englert, M. Bolte, H.-W. Lerner, M. C. Holthausen and M. Wagner, Main-Chain Boron-Containing Oligophenylenes via Ring-Opening Polymerization of 9-H-9-Borafluorene, *J. Am. Chem. Soc.*, 2011, **133**, 4596–4609; (b) Y. Shoji, N. Tanaka, S. Muranaka, N. Shigeno, H. Sugiyama, K. Takenouchi, F. Hajjaj and T. Fukushima, Boron-mediated sequential alkyne insertion and C–C coupling reactions affording extended π -conjugated molecules, *Nat. Commun.*, 2016, **7**, 12704; (c) K. R. Bluer, L. E. Laperriere, A. Pujol, S. Yruegas, V. A. K. Adiraju and C. D. Martin, Coordination and Ring Expansion of 1,2-Dipolar Molecules with 9-Phenyl-9-borafluorene, *Organometallics*, 2018, **37**, 2917–2927; (d) Y. Murata, K. Matsunagi, J. Kashida, Y. Shoji, C. Özen, S. Maeda and T. Fukushima, Observation of Borane–Olefin Proximity Interaction Governing the Structure and Reactivity of Boron-Containing Macrocycles, *Angew. Chem., Int. Ed.*, 2021, **60**, 14630–14635; (e) T. Bischof, X. Guo, I. Krummenacher, L. Beßler, Z. Lin, M. Finze and H. Braunschweig, Alkene insertion reactivity of a *o*-carbora-nyl-substituted 9-borafluorene, *Chem. Sci.*, 2022, **13**, 7492–7497.
- 9 For selected publications on alumoles, the non-benzannulated congeners of AlFlus, see: (a) H. Hoberg and R. Krause-Göing, Darstellung und Eigenschaften von Pentaphenylaluminacyclopentadien, *J. Organomet. Chem.*, 1977, **127**, C29–C31; (b) T. Wasano, T. Agou, T. Sasamori and N. Tokitoh, Synthesis, structure and reactivity of a 1-bromoalumole, *Chem. Commun.*, 2014, **50**, 8148–8150; (c) T. Agou, T. Wasano, T. Sasamori and N. Tokitoh, Syntheses and Structures of Stable 1-Aminoalumole Derivatives, *Organometallics*, 2014, **33**, 6963–6966; (d) Y. Zhang, J. Wei, W.-X. Zhang and Z. Xi, Lithium Aluminate Complexes and Alumoles from 1,4-Dilithio-1,3-Butadienes and AlEt₂Cl, *Inorg. Chem.*, 2015, **54**, 10695–10700; (e) N. Tokitoh, T. Agou, T. Wasano and T. Sasamori, Synthesis and properties of stable alumoles, *Phosphorus, Sulfur, Silicon Relat. Elem.*, 2016, **191**, 584–587; (f) V. Y. Lee, H. Sugawara, O. A. Gapurenko, R. M. Minyaev, V. I. Minkin, H. Gornitzka and A. Sekiguchi, 1-Chloroalumole, *Organometallics*, 2022, **41**, 467–471.
- 10 T. Agou, T. Wasano, P. Jin, S. Nagase and N. Tokitoh, Syntheses and Structures of an “Alumole” and Its Dianion, *Angew. Chem., Int. Ed.*, 2013, **52**, 10031–10034.
- 11 (a) T. D. Coyle, S. L. Stafford and F. G. A. Stone, Chemical and Spectroscopic Evidence for the Occurrence of π -Character in Carbon–Boron Bonds, *J. Chem. Soc.*, 1961, 3103–3108; (b) A. Foord, B. Beagley, W. Reade and I. A. Steer, A gas-phase electron-diffraction study of trivinylborane, *J. Mol. Struct.*, 1975, **24**, 131–137; (c) Y. Yamamoto and I. Moritani, Carbon-13 Nuclear Magnetic Resonance Studies of Organoboranes. The Relative Importance of Mesomeric B–C π -Bonding Forms in Alkenyl- and Alkynylboranes, *J. Org. Chem.*, 1975, **40**, 3434–3437.
- 12 J. J. Eisch and W. C. Kaska, The Novel Synthesis of Aluminols by the Metalative Cyclization of Unsaturated Organoaluminum Compounds, *J. Am. Chem. Soc.*, 1962, **84**, 1501–1502.
- 13 J. J. Eisch and W. C. Kaska, The Synthesis of Aluminols via the Addition and Cyclization Reactions of Arylaluminum Compounds, *J. Am. Chem. Soc.*, 1966, **88**, 2976–2983.
- 14 T. Matsumoto, H. Takamine, K. Tanaka and Y. Chujo, Synthesis and Characterization of Heterofluorenes with Five-coordinated Group 13 Elements, *Chem. Lett.*, 2015, **44**, 1658–1660.
- 15 T. Matsumoto, K. Tanaka, K. Tanaka and Y. Chujo, Synthesis and characterization of heterofluorenes containing four-coordinated group 13 elements: theoretical and experimental analyses and comparison of structures, optical properties and electronic states, *Dalton Trans.*, 2015, **44**, 8697–8707.
- 16 R. Drescher, L. Wüst, C. Mihm, I. Krummenacher, A. Hofmann, J. Goettel and H. Braunschweig, Synthesis, structure and insertion reactivity of Lewis acidic 9-aluminafluorenes, *Dalton Trans.*, 2021, **50**, 10400–10404.
- 17 We are aware that the compounds AlMe₃ and AlBr₃ are monomeric neither in solution nor in the solid state. However, for simplicity, the monomeric forms were used in calculating the quantities employed.
- 18 P. L. Lückert, J. Gilmer, A. Virovets, H.-W. Lerner and M. Wagner, Donor-free 9,10-dihydro-9,10-dialuminaanthracenes, *Chem. Sci.*, DOI: [10.1039/D4SC06940D](https://doi.org/10.1039/D4SC06940D).
- 19 SnMe₄ can in principle be recovered and used to recycle the Me₂SnCl₂ required to synthesize **1**.
- 20 Two polymorphs of (Me–AlFlu)₂ have been structurally characterized by X-ray diffraction: The denser α -form crystallizes in the triclinic space group *P* $\bar{1}$ with one unique molecule at a general position and a second molecule at an inversion center (*Z* = 3). The β -form, which is discussed in the main text, crystallizes in the monoclinic space group *P*2₁/*n* with one crystallographically unique molecule at an inversion center. The key structural parameters of all the molecules are essentially identical (Fig. S39†); full details are available in the ESI.†
- 21 A. Hübner, M. Diefenbach, M. Bolte, H.-W. Lerner, M. C. Holthausen and M. Wagner, Confirmation of an Early Postulate: B–C–B Two-Electron–Three-Center Bonding in Organo(hydro)boranes, *Angew. Chem., Int. Ed.*, 2012, **51**, 12514–12518.
- 22 C. Elschenbroich, *Organometallics*, WILEY-VCH, Weinheim, Germany, 2006.



- 23 M. A. Fox and J. K. Whitesell, *Organic Chemistry*, Jones and Bartlett, Sudbury, Massachusetts, USA, 2003, p. 77.
- 24 E. D. Glendening, R. Faust, A. Streitwieser, K. P. C. Vollhardt and F. Weinhold, The Role of Delocalization in Benzene, *J. Am. Chem. Soc.*, 1993, **115**, 10952–10957.
- 25 The molecular structure of 2-OEt₂ was excluded from this comparison due to its significantly larger error margins.
- 26 (a) M. Karplus and J. A. Pople, Theory of Carbon NMR Chemical Shifts in Conjugated Molecules, *J. Chem. Phys.*, 1963, **38**, 2803–2807; (b) R. H. Levin and J. D. Roberts, Nuclear magnetic resonance spectroscopy. Ring-current effects upon carbon-13 chemical shifts, *Tetrahedron Lett.*, 1973, **24**, 135–138; (c) H. Günther, H. Schmickler, H. Königshofen, K. Recker and E. Vogel, Does a “Ring Current Effect” Exist for ¹³C-Nuclear Magnetic Resonance? A Study of Bridged Annulenes, *Angew. Chem., Int. Ed.*, 1973, **12**, 243–245; (d) D. G. Farnum, Charge Density-NMR Chemical Shift Correlations in Organic Ions, *Adv. Phys. Org. Chem.*, 1975, **11**, 123–175.
- 27 (a) A. Schnurr, M. Bolte, H.-W. Lerner and M. Wagner, Cyclic Phosphonium Bis(fluoroaryl)boranes – Trends in Lewis Acidities and Application in Diels–Alder Catalysis, *Eur. J. Inorg. Chem.*, 2012, 112–120; (b) M. Henkelmann, A. Omlor, M. Bolte, V. Schünemann, H.-W. Lerner, J. Noga, P. Hrobárik and M. Wagner, A free boratriptycene-type Lewis superacid, *Chem. Sci.*, 2022, **13**, 1608–1617.
- 28 ¹³C{¹H} NMR data (the numbering scheme used here differs from that used in the ESI†): 147.3 (C-2,6), 125.0 (C-3,5), 139.9 (C-4) for 2-py; 149.1 (C-2,6), 124.3 (C-3,5), 137.8 (C-4) for 4-py; 148.3 (C-2,6), 125.6 (C-3,5), 141.0 (C-4) for BPh₃·py. X-ray analysis: Al–N = 1.9969(16)/2.0160(17) Å, N–Al–COG = 105.44/112.06° for two crystallographically independent molecules of 2-py. Al–N = 1.964(2) Å, N–Al–COG = 122.26° for 4-py. COG: centroid of the AlC₄ heterocycle.
- 29 H. Budy, S. E. Prey, C. D. Buch, M. Bolte, H.-W. Lerner and M. Wagner, Nucleophilic borylation of fluorobenzenes with reduced arylboranes, *Chem. Commun.*, 2022, **58**, 254–257.

